

Theoretical Analysis of Dipole Moment Derivatives in Fluoromethanes.

(II) Difluoromethane

Kwan Kim

Department of Chemistry, College of Natural Sciences, Seoul National University, Seoul 151

Received September 30, 1986

The results of an ab initio (6-31G) molecular orbital calculation of the dipole moment derivatives and gas phase IR intensities of difluoromethane are reported. The results are compared with corresponding values obtained from a CNDO calculation. The directions of the dipole derivatives calculated by the two methods agree very well, whereas the intensities differ significantly. The results are also analyzed for the charge-charge flux-overlap electronic contributions to the dipole derivatives.

Introduction

A number of reasonably successful predictions have been made for the infrared intensities of the fundamental absorption bands for molecules containing fluorine atoms, using a F-atom polar tensor transferred from the experimental polar tensor derived from the CH₃F molecule^{1,2}. However, it has been reported by Newton et al.³ that the calculated intensities of CH₂F₂ by using the hydrogen and fluorine tensors transferred from CH₃F deviate somewhat significantly from the experimental data.

Morcillo et al.⁴ have previously interpreted the experimental infrared intensities of CH₂F₂. However, they were not able to decide which of the several possible sets of atomic polar tensors (arising from different choices of signs for the $\partial P/\partial Q_i$ derivatives) were correct.

Following the above implications, we have performed the quantum mechanical analysis for the infrared intensities of fundamental vibrations of difluoromethane (CH₂F₂ and CD₂F₂); the results are presented here.

Method of Calculation

The intensities of the fundamentals are calculated by making use of the concept of the atomic polar tensors. The polar tensor for an atom α in a molecule is defined as⁵

$$P_x^\alpha = \begin{bmatrix} \partial P_x/\partial x_\alpha & \partial P_x/\partial y_\alpha & \partial P_x/\partial z_\alpha \\ \partial P_y/\partial x_\alpha & \partial P_y/\partial y_\alpha & \partial P_y/\partial z_\alpha \\ \partial P_z/\partial x_\alpha & \partial P_z/\partial y_\alpha & \partial P_z/\partial z_\alpha \end{bmatrix} \quad (1)$$

Here P_x , etc., is the x component of the dipole moment and x_α , y_α , etc., are the space-fixed Cartesian coordinates locating the α atom.

The detailed description of how the fundamental intensities are derived from the atomic polar tensors (or vice versa) is given elsewhere⁶. Briefly, once the atomic polar tensors (APT's) are given in the correct molecular coordinate frames, the P_Q matrix (composed of the Cartesian components of the dipole moment derivatives with respect to the normal coordinates) is calculated by⁵

$$P_Q = P_x A L \quad (2)$$

Here P_x is the $3 \times 3n$ (n = the number of atoms) matrix composed of the n juxtaposed 3×3 APT's, A is the symmetrized A matrix (the inverse of the Wilson's B matrix), and L is the symmetrized normal coordinate transformation matrix⁵. The integrated band area is related to the P_Q elements, $\partial P/\partial Q_i$, by⁷

$$A_i = (974.8644) (\partial P/\partial Q_i)^2 (\text{Km mole}^{-1}), \quad (3)$$

if $\partial P/\partial Q_i$ is in eu⁻¹. (Here u designates atomic mass units, and e is the charge on the electron: $1e = 1.602 \times 10^{-19}$ C.)

To calculate the elements of the APT's the numerical differentiation approximation $\partial P/\partial \sigma \approx \Delta P/\Delta \sigma$ is employed, with $\Delta \sigma = 0.02$ Å. The calculations have been performed by the

Table 1. Structural Data and Definition of Internal and Symmetry Coordinates of Difluoromethane

Masses(u): $m_C = 12.0$, $m_H = 1.007825$, $m_F = 2.014102$.

$m_r = 18.998405$

Structure⁸: $R_{C-F} = 0.10934$ nm, $R_{C-F} = 0.13574$ nm,

$H\hat{C}H = 113^\circ 40'$, $F\hat{C}F = 108^\circ 19'$

Dipole: 6.571×10^{-30} C·m

Internal coordinates⁹: $R_1 = \delta r_{12}$, $R_6 = \delta \alpha_{415}$
 $R_2 = \delta r_{13}$, $R_7 = \delta \alpha_{214}$
 $R_3 = \delta r_{14}$, $R_8 = \delta \alpha_{215}$
 $R_4 = \delta r_{15}$, $R_9 = \delta \alpha_{314}$
 $R_5 = \delta \alpha_{213}$, $R_{10} = \delta \alpha_{315}$

Symmetry coordinates:

$S_1 = (1/\sqrt{2})(R_1 + R_2)$
 $S_2 = (1/\sqrt{2})(R_3 + R_4)$
 A_1 $S_3 = aR_5 - b(R_7 + R_8 + R_9 + R_{10})$
 $S_4 = cR_6 - dR_5 - e(R_7 + R_8 + R_9 + R_{10})$
 A_2 $S_5 = (1/2)(R_7 - R_8 - R_9 + R_{10})$
 $S_6 = (1/\sqrt{2})(R_1 - R_2)$
 B_1 $S_7 = (1/2)(R_3 + R_4 - R_9 - R_{10})$
 $S_8 = (1/\sqrt{2})(R_3 - R_4)$
 B_2 $S_9 = (1/2)(R_7 - R_8 + R_9 - R_{10})$
 A_1 $S_{red} = fR_3 + gR_6 + h(R_7 + R_8 + R_9 + R_{10})$
 $a = 0.88815$, $b = 0.22977$
 $c = 0.92336$, $d = 0.17643$, $e = 0.17049$
 $f = 0.42433$, $g = 0.38393$, $h = 0.41005$

⁸Reference 11. ⁹Reference 12. ¹⁰Reference 13. ¹¹The subscripts refer to the atoms shown in Figure 1(a); r_{ij} and α_{ijk} represent, respectively, the appropriate bond-length and bond-angle. ¹²The symmetry type was classified based on the C_{2v} point group. S_{red} represents the redundancy condition.

Table 2. Harmonic Force Field and Normal Coordinates of Difluoromethane

Harmonic force constants (Nm ⁻¹):				
A ₁	K ₁₁ = 537.7, K ₁₂ = 35.6, K ₂₂ = 693.8, K ₁₃ = 10.9, K ₁₃ = -34.4,			
	K ₃₃ = 62.0, K ₁₄ = -4.4, K ₂₄ = 36.7, K ₃₄ = -3.3, K ₄₄ = 137.7			
A ₂	K ₅₅ = 77.2			
B ₁	K ₆₆ = 529.4, K ₆₇ = 17.6, K ₇₇ = 115.6			
B ₂	K ₈₈ = 523.6, K ₈₉ = 80.9, K ₉₉ = 92.7			
Normal coordinates (u ^{-1/2}):				
CH ₂ F ₂	Q ₁	Q ₂	Q ₃	Q ₄
A ₁ S ₁	1.02052	-0.02511	-0.00066	-0.00454
S ₂	-0.05023	0.06793	0.31685	0.04741
S ₃	-0.05526	1.50936	-0.02295	0.06741
S ₄	0.08020	-0.11172	-0.29280	0.31907
	Q ₅			
A ₂ S ₅	1.12256			
	Q ₆	Q ₇		
B ₁ S ₆	1.05310	0.00212		
S ₇	-0.17220	0.85750		
	Q ₈	Q ₉		
B ₂ S ₈	-0.09361	0.39166		
S ₉	1.23150	-0.18598		
CD ₂ F ₂	Q ₁	Q ₂	Q ₃	Q ₄
A ₁ S ₁	0.73872	0.01602	-0.01903	-0.00730
S ₂	-0.08236	0.24509	-0.20241	0.04422
S ₃	-0.12968	0.88833	0.64845	0.09232
S ₄	0.12526	-0.27215	0.12954	0.31608
	Q ₅			
A ₂ S ₅	0.80799			
	Q ₆	Q ₇		
B ₁ S ₆	0.78269	0.02600		
S ₇	-0.25236	0.69228		
	Q ₈	Q ₉		
B ₂ S ₈	0.33410	0.22481		
S ₉	-0.86315	0.44594		

*Reference 10. *The indices labelling the normal coordinates correspond to the labels identifying the vibrational mode given in reference 10.

CNDO^a and ab initio methods. The ab initio calculations were carried out with the GAUSSIAN-70 program⁹ using the 6-31G basis set. Experimental values are used both for the molecular geometry and for the force field. The equilibrium structural data and the definition of the internal and symmetry coordinates are listed in Table 1. The normal coordinates calculated using the force field given by Blom and Müller¹⁰ are given in Table 2. The coordinate axes and molecular orientation of difluoromethane used in the normal coordinate calculation are shown in Figure 1(a).

Table 3. Calculated intensities of CH₂F₂ and CD₂F₂ in the units of km mole⁻¹ s

	Band	ν_i (cm ⁻¹)	6-31G	CNDO	Observed ^a	
CH ₂ F ₂	A ₁	ν_1	2948	35.0	29.5	29.8
		ν_2	1508	3.1	11.6	0
		ν_3	1113	130	61.2	55.0
		ν_4	528	12.7	11.0	4.7
	A ₂	ν_5	1262	0	0	0
	B ₁	ν_6	3014	63.8	53.8	41.0
		ν_7	1178	31.5	37.2	8.95
		ν_8	1435	24.9	30.0	10.3
	B ₂	ν_9	1090	218	106	243.9
CD ₂ F ₂	A ₁ , B ₂	ν_1	2129	38.5	29.6	15.3
		ν_2	1165	245.5	166	172.5
	ν_8	1158				
	ν_3	1027				
		ν_9	1002	105.2	32.7	113.5
		ν_4	522	13.1	10.8	4.9
	A ₂	ν_5	907	0	0	0
B ₁	ν_6	2284	56.5	47.5	18.2	
	ν_7	962	32.8	33.2	7.8	

*Reference 14.

Results and Discussion

The intensities calculated for the fundamental vibrations of CH₂F₂ and CD₂F₂ are compared with the experimental values in Table 3. The calculated intensities are, in general, higher than the experimental values, approximately by a factor of 2. The most noticeable disagreement occurs for the 1508 cm⁻¹ CH₂ scissor mode (ν_2) of CH₂F₂. The measured intensity is zero (or very, very small). We predict a nonzero intensity for this mode. The ab initio calculated intensity appears to be more reasonable than the CNDO result.

For the relative intensities of the symmetric CF₂ stretching mode (ν_3), the CH₂ rocking mode (ν_7), and the CF₂ asymmetric stretching mode (ν_9) in CH₂F₂, there are some discrepancies between calculated and experimental results. The measured relative intensities of the ν_3 and ν_7 bands with respect to that of the intense ν_9 band were substantially smaller. It is possible that those discrepancies arise from the difficulty in separating the overlapped bands experimentally. The ν_3 mode is indeed overlapped by the intense ν_9 mode and by the weak ν_7 mode. It can be seen from Table 3 that the agreement between the experimental and calculated intensities of CH₂F₂ is much better when they are summed over all the bands in the 1100 cm⁻¹ spectral region.

For CD₂F₂, the most noticeable discrepancy between experimental and calculated intensities occurs for the B₁ modes. The calculated intensities of ν_1 and ν_4 modes are about two times larger than the measured values. It is noteworthy that the CNDO calculated intensities of the CF₂ asymmetric stretching mode (ν_9) in both molecules, CH₂F₂ and CD₂F₂, are too small. On the other hand, the intensities of the CH stretching modes (ν_1 and ν_4) are overestimated by this method. In this regard, the ab initio method appears to be superior to the semiempirical method. In order to gain more information on

Table 4. Atomic polar tensors of difluoromethane in units of e^2s

	C(1)	H(2)	F(4)
6-31G	$\begin{bmatrix} 0.996 & 0 & 0 \\ 0 & 1.508 & 0 \\ 0 & 0 & 1.238 \end{bmatrix}$	$\begin{bmatrix} -0.114 & 0 & -0.048 \\ 0 & -0.019 & 0 \\ -0.086 & 0 & -0.018 \end{bmatrix}$	$\begin{bmatrix} -0.384 & 0 & 0 \\ 0 & -0.735 & 0.268 \\ 0 & 0.196 & -0.601 \end{bmatrix}$
CNDO	$\begin{bmatrix} 0.900 & 0 & 0 \\ 0 & 1.130 & 0 \\ 0 & 0 & 0.990 \end{bmatrix}$	$\begin{bmatrix} -0.123 & 0 & -0.018 \\ 0 & -0.055 & 0 \\ -0.057 & 0 & -0.064 \end{bmatrix}$	$\begin{bmatrix} -0.327 & 0 & 0 \\ 0 & -0.510 & 0.155 \\ 0 & 0.056 & -0.431 \end{bmatrix}$
Expt'l	$\begin{bmatrix} 0.681 & 0 & 0 \\ 0 & 1.495 & 0 \\ 0 & 0 & 0.800 \end{bmatrix}$	$\begin{bmatrix} -0.087 & 0 & -0.061 \\ 0 & 0.020 & 0 \\ -0.101 & 0 & -0.011 \end{bmatrix}$	$\begin{bmatrix} -0.253 & 0 & 0 \\ 0 & -0.767 & 0.378 \\ 0 & 0.142 & -0.389 \end{bmatrix}$
CH ₂ F ^a	$\begin{bmatrix} 0.716 & 0 & 0 \\ 0 & 1.256 & 0 \\ 0 & 0 & 1.031 \end{bmatrix}$	$\begin{bmatrix} -0.103 & 0 & -0.082 \\ 0 & 0.073 & 0 \\ -0.054 & 0 & -0.028 \end{bmatrix}$	$\begin{bmatrix} -0.255 & 0 & 0 \\ 0 & -0.701 & 0.322 \\ 0 & 0.322 & -0.489 \end{bmatrix}$

^aAPT's of CH₂F₂ correspond to those of atoms numbered in Figure 1(a). ^bPolar tensors reported in reference (16) are transformed in accordance with the coordinate system shown in Figure 1(b).

the cause of underestimation of the ν_3 band intensities, the CNDO results are analyzed for the charge-charge flux-overlap electronic contributions to the dipole derivatives. Those results will be discussed later.

According to the ab initio calculations, the ν_2 band for CD₂F₂ contributes 24% to the overlapped $\nu_2 + \nu_6$ band and the ν_3 band 46% to the overlapped $\nu_3 + \nu_6$ band. For their verification, spectra should be taken at low temperature. Nevertheless, it may be appropriate to mention that, as will be discussed later, the reported intensities of CH₂F₂ and CD₂F₂ seem not to be isotopically consistent with each other.

The calculated APTs for the C(1), H(2), and F(4) atoms in Figure 1(a) are listed in Table 4. Although the magnitudes of the APT elements are not exactly consistent between the two calculations, the general trends are in fair agreement. In specific, the signs of the elements obtained from the semi empirical method agree well with those from the ab initio method. Moreover, the two methods have resulted in the same signs for the dipole derivatives with respect to the normal coordinates, $\partial P_i/\partial Q_j$. For difluoromethane which belongs to the C_{2v} point group, $\partial P_i/\partial Q_j$'s are the only nonzero elements for the A₁ vibrational modes, $\partial P_i/\partial Q_j$'s for the B₁ modes, and $\partial P_i/\partial Q_j$'s for the B₂ modes in the coordinates defined in Figure 1(a). Theoretical calculations led to the (- + + -) choice of signs for the A₁ modes of CH₂F₂ ($\partial P_i/\partial Q_1$ and $\partial P_i/\partial Q_2$ being negative and the others positive). The (- +) ($\partial P_i/\partial Q_3$ being negative and $\partial P_i/\partial Q_4$ positive) and (+ -) ($\partial P_i/\partial Q_5$ being positive and $\partial P_i/\partial Q_6$ negative) signs were unequivocally obtained for the B₁ and B₂ modes, respectively, in CH₂F₂. For CD₂F₂, the (- + - -), (- +) and (- -) sign sets were obtained for the A₁, B₁, and B₂ modes, respectively.

Since both theoretical calculations have led to the same sign choices for the dipole derivatives of difluoromethane with respect to the normal coordinates, we have derived the atomic polar tensors from the reported intensities of CH₂F₂ on the basis of signs calculated quantum mechanically. The results are also listed in Table 4. It appears that the APTs obtained in this way correlate better with the ab initio results. The one noticeable exception occurred for the YY component of the H(2) APT. There exists sign discrepancy between the experimental and calculated APTs. However, it should be

pointed out that the kind of discrepancy found here may have arisen because of the difficulty in separating the overlapped intensities experimentally. In order to test such a possibility we have calculated the intensities of CD₂F₂ by using the APTs obtained from the experimental intensities of CH₂F₂. Assuming that the sign choices taken from the quantum mechanical calculations are correct, the predicted intensities of CD₂F₂ should be in close agreement with the measured values. The predicted intensities are 26.2, 196.1, 106.3, 4.9, 33.1, and 10.7 km/mole for the ν_1 , $\nu_2 + \nu_6$, $\nu_3 + \nu_6$, ν_4 , ν_5 , and ν_7 modes of CD₂F₂, respectively. We see that there are indeed some discrepancies between calculated and experimental intensities. The major discrepancy appears to be in the intensities of the CD stretching modes, ν_1 and ν_6 (predicted: 26.2, experimental: 15.3 km/mole for ν_1 and predicted: 33.1 experimental 18.2 km/mole for ν_6). At this time we are not able to judge which of two sets, predicted and experimental, is correct. In this respect, it may be worthwhile to remeasure the infrared intensities of the fundamental bands in both molecules of CH₂F₂.

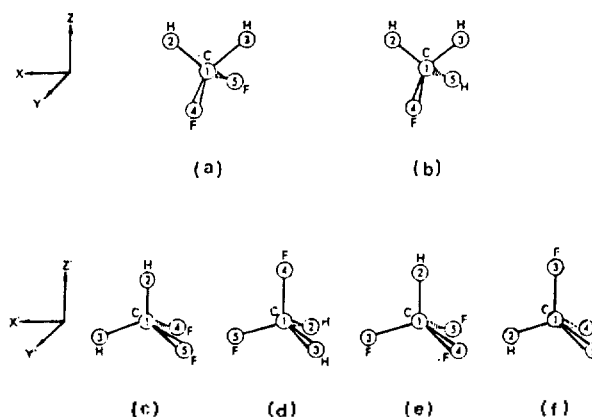


Figure 1. (a) Coordinate axes of difluoromethane used in the normal coordinate calculation; (b) Coordinate axes of CH₂F correlating with (a); (c) & (d) Rotated coordinate systems of CH₂F₂ with the z' axes along the respective C-H(2) and C-F(4) bonds; (e) & (f) Rotated coordinate systems of CHF, with the z' axes along the respective C-H(2) and C-F(3) bonds.

and CD_2F_2 . Nevertheless, it would be interesting to notice that the predicted intensities of the ν_1 and ν_8 modes in CD_2F_2 above are closer to the quantum mechanically calculated values.

The rotated $P_x^{(1)}$, $P_x^{(2)}$, and $P_x^{(4)}$ tensors of CH_3F after conversion to the coordinate system for difluoromethane (see Figure 1(b)) are also listed in Table 4. As mentioned earlier, Person et al.³ used the APTs of CH_3F in the prediction of the intensities of CH_2F_2 and found that the agreement between the observed and calculated intensities is not as good as expected in light of the generally good agreement obtained for other systems. It can be seen from Table 4 that the absolute values of the yy and yz elements of $P_x^{(4)}$ transferred from CH_3F are significantly smaller than those from CH_2F_2 , rendering the yy element of $P_x^{(4)}$ being relatively smaller. Accordingly, the predicted intensities for the B_2 modes turned out to be substantially smaller than the observed data. On the other hand, the absolute values of the zy and zz elements of $P_x^{(4)}$ from CH_3F are larger than those from CH_2F_2 , resulting in the relatively larger value for the zz element of $P_x^{(4)}$. These effects seem to have led to the predicted intensities of the A_1 modes of CH_2F_2 being larger than the experimental intensities.

We have no easy explanation for the discrepancies between the predicted and experimental intensities. Nevertheless it appears that the neighbor (H-H, H-F, and F-F) interactions should be considered for interpreting the difference between the APTs of related molecules. For the quantitative rationalization, more systematic studies should be performed.

In order to get more information on the electronic structure changes taking place during vibrational motions, the quantum mechanical polar tensors are analyzed for the charge-charge flux-overlap (CCFO) electronic contributions¹⁵. The results are represented in Table 5. The $P_x^{(2)}$ and $P_x^{(4)}$ tensors are given in coordinate systems with the z' axes along the C-H(2) and C-F(4) bonds as shown in Figure 1(c) and 1(d), respectively, for comparison with those of CHF_3 . The $P_x^{(2)}$ and $P_x^{(4)}$ tensors of CHF_3 correspond to the coordinate systems shown in Figure 1(e) and 1(f), respectively.

The major discrepancy between semi-empirical and ab initio calculated tensors arises from the differences in the net charge contributions. The net charge effect estimated from the ab initio method is considerably larger than that from the semi-empirical method. On the other hand, the charge flux contributions from both methods are much the same. It thus appears that underestimation of the CNDO calculation for the ν_8 band intensities of CH_2F_2 and CD_2F_2 arises from the relatively smaller net charge contributions.

It seems interesting to notice that the net charge contributions are nearly the same for both molecules, difluoromethane and fluoroform. The ab initio calculations exhibit that as the C-F bond stretches out the dipole component of CHF_3 perpendicular to the stretching motion is greatly affected by the charge flux contribution compared to that in CH_2F_2 . Such a large charge transfer effect is, however, compensated by the quantum mechanical interference effect letting the APTs of both molecules being comparable.

In order to assess the relative importance of each of three CCFO contributions for a given tensor we may define the following quantity,

$$\xi_a^2 = (1/3) \sum_{\alpha} [(\partial P_{\alpha} / \partial x_{\alpha})^2 + (\partial P_{\alpha} / \partial y_{\alpha})^2 + (\partial P_{\alpha} / \partial z_{\alpha})^2] \quad (4)$$

as the square of the "effective term-charge". According to

the ab initio calculations, the effective term-charges of hydrogen atom in CH_2F_2 are 0.17, 0.09, and 0.16 e, respectively, for the net charge, charge flux, and overlap contributions. The corresponding values in CHF_3 are 0.20, 0.09, and 0.20 e. For fluorine atom, the effective term-charges are 0.42, 0.30, and 0.07 e in CH_2F_2 and 0.38, 0.37, and 0.26 e in CHF_3 , for the net charge, charge flux, and overlap contributions, respectively. From the standpoint of ab initio calculations, it thus appears that the quantum mechanical interference effect increases as one H-atom of CH_2F_2 is replaced with a F-atom. It can also be seen that the charge-flux term is less important in the H-atom polar tensors while that becomes a dominant term for the F-atom tensors.

In the CNDO limit, somewhat different behaviors are observed. The effective term-charges of hydrogen atom are 0.01, 0.08, and 0.06 e in CH_2F_2 and 0.02, 0.08, and 0.04 e in CHF_3 for the net charge, charge flux, and overlap contributions, respectively. For the fluorine atom, the corresponding values are 0.20, 0.21, and 0.09 e for CH_2F_2 and 0.20, 0.23, and 0.11 e for CHF_3 . It seems interesting to notice that the values of effective term-charges in both molecules are much the same. The charge flux contribution plays dominant role for two atoms, H and F, in both molecules, CH_2F_2 and CHF_3 .

Finally, it may also be interesting to compare the calculated effective atomic charges with those obtained from the analysis of the measured intensities. The square of the effective atomic charge is defined as one-third of the sum of squares of the polar tensor components; that is¹⁷,

$$\chi_a^2 \equiv (1/3) \text{Tr} (P_{\alpha}^{\alpha} P_{\alpha}^{\alpha}) \quad (5)$$

The hydrogen atom effective charge in CH_2F_2 was found to be 0.09 e from the analysis of measured intensities. Both the ab initio and CNDO calculations gave the same values. The ab initio and CNDO calculated values for the fluorine atom effective charge of CH_2F_2 are 0.62 and 0.44 e, respectively. The observed value, 0.57 e, agrees better with the ab initio result. Similar behavior was observed in the case of CHF_3 . The ab initio calculated effective charges of H and F atoms in CHF_3 are in good agreement with the observed values whereas the CNDO results exhibit substantial discrepancies. The ab initio calculated effective charges for the fluorine atoms in CH_2F_2 and CHF_3 are exactly the same. Thus, the effective fluorine charge appears to be insensitive to the molecular structure. On the other hand, the effective hydrogen charge of CH_2F_2 differs significantly from the value (6-31G: 0.05, CNDO: 0.11, obs: 0.05 e) of CHF_3 . However, the value for CH_2F_2 falls inside of the range, $\chi_{H}/e = 0.088 \pm 0.015$, observed for most hydrocarbons².

In conclusion, we have performed ab initio and semi-empirical calculations for the dipole moment derivatives of difluoromethane. The two methods have resulted in the same signs for the dipole derivatives with respect to the normal coordinates. The calculated intensities were, in general, larger than the observed values, approximately by a factor of 2. It seemed to be prudent to remeasure the intensities for both isotopically related molecules, CH_2F_2 and CD_2F_2 . We have also analyzed the theoretical polar tensors into the charge-charge flux-overlap contributions. The major discrepancy between semi-empirical and ab initio calculated tensors seemed to arise from the differences in the net charge contributions. In addition, the effective fluorine charge appeared not to be sensitive

Table 5. The CNDO and ab Initio Atomic Polar Tensors of CH₃F, and CHF₃, Analyzed for the Charge-Charge Flux-Overlap Contributions to the Dipole Derivatives (units of e)

		APTs	CCFO contributions								
			net charge			charge-flux			overlap		
CH ₃ F ^a	6-31G	$P_{\nu}^{\mu(2)} = \begin{bmatrix} 0.02 & 0 & -0.00 \\ 0 & -0.02 & 0 \\ 0.04 & 0 & -0.15 \end{bmatrix}$	$\begin{bmatrix} 0.17 & 0 & 0 \\ 0 & 0.17 & 0 \\ 0 & 0 & 0.17 \end{bmatrix}$	$\begin{bmatrix} -0.07 & 0 & -0.01 \\ 0 & -0.11 & 0 \\ -0.02 & 0 & -0.08 \end{bmatrix}$	$\begin{bmatrix} -0.09 & 0 & 0.00 \\ 0 & -0.08 & 0 \\ 0.06 & 0 & -0.24 \end{bmatrix}$						
		$P_{\nu}^{\nu(2)} = \begin{bmatrix} -0.43 & 0 & 0.03 \\ 0 & -0.38 & 0 \\ -0.05 & 0 & -0.91 \end{bmatrix}$	$\begin{bmatrix} -0.42 & 0 & 0 \\ 0 & -0.42 & 0 \\ 0 & 0 & -0.42 \end{bmatrix}$	$\begin{bmatrix} -0.05 & 0 & -0.03 \\ 0 & -0.03 & 0 \\ 0.03 & 0 & -0.52 \end{bmatrix}$	$\begin{bmatrix} 0.04 & 0 & 0.05 \\ 0 & 0.06 & 0 \\ -0.07 & 0 & 0.03 \end{bmatrix}$						
	CNDO	$P_{\nu}^{\mu(2)} = \begin{bmatrix} -0.05 & 0 & -0.01 \\ 0 & -0.06 & 0 \\ 0.03 & 0 & -0.14 \end{bmatrix}$	$\begin{bmatrix} -0.01 & 0 & 0 \\ 0 & -0.01 & 0 \\ 0 & 0 & -0.01 \end{bmatrix}$	$\begin{bmatrix} -0.09 & 0 & 0.00 \\ 0 & -0.07 & 0 \\ -0.02 & 0 & -0.07 \end{bmatrix}$	$\begin{bmatrix} 0.05 & 0 & -0.01 \\ 0 & 0.02 & 0 \\ 0.05 & 0 & -0.06 \end{bmatrix}$						
		$P_{\nu}^{\nu(2)} = \begin{bmatrix} -0.36 & 0 & 0.05 \\ 0 & -0.33 & 0 \\ -0.05 & 0 & -0.58 \end{bmatrix}$	$\begin{bmatrix} -0.20 & 0 & 0 \\ 0 & -0.20 & 0 \\ 0 & 0 & -0.20 \end{bmatrix}$	$\begin{bmatrix} -0.04 & 0 & 0.04 \\ 0 & -0.05 & 0 \\ 0.01 & 0 & -0.36 \end{bmatrix}$	$\begin{bmatrix} -0.12 & 0 & 0.02 \\ 0 & -0.08 & 0 \\ -0.05 & 0 & -0.03 \end{bmatrix}$						
	Expt'l	$P_{\nu}^{\mu(2)} = \begin{bmatrix} 0.04 & 0 & -0.02 \\ 0 & 0.02 & 0 \\ 0.02 & 0 & -0.14 \end{bmatrix}$									
		$P_{\nu}^{\nu(2)} = \begin{bmatrix} -0.27 & 0 & 0.22 \\ 0 & -0.25 & 0 \\ -0.02 & 0 & -0.88 \end{bmatrix}$									
	6-31G	$P_{\nu}^{\mu(2)} = \begin{bmatrix} -0.01 & 0 & 0 \\ 0 & -0.01 & 0 \\ 0 & 0 & -0.08 \end{bmatrix}$	$\begin{bmatrix} 0.02 & 0 & 0 \\ 0 & 0.20 & 0 \\ 0 & 0 & 0.20 \end{bmatrix}$	$\begin{bmatrix} -0.11 & 0 & 0 \\ 0 & -0.11 & 0 \\ 0 & 0 & 0.04 \end{bmatrix}$	$\begin{bmatrix} -0.10 & 0 & 0 \\ 0 & -0.10 & 0 \\ 0 & 0 & -0.31 \end{bmatrix}$						
		$P_{\nu}^{\nu(2)} = \begin{bmatrix} -0.42 & 0 & -0.07 \\ 0 & -0.44 & 0 \\ 0.04 & 0 & -0.89 \end{bmatrix}$	$\begin{bmatrix} -0.38 & 0 & 0 \\ 0 & -0.38 & 0 \\ 0 & 0 & -0.38 \end{bmatrix}$	$\begin{bmatrix} -0.08 & 0 & 0.37 \\ 0 & -0.08 & 0 \\ -0.04 & 0 & -0.52 \end{bmatrix}$	$\begin{bmatrix} 0.04 & 0 & -0.44 \\ 0 & 0.03 & 0 \\ 0.09 & 0 & 0.01 \end{bmatrix}$						
CHF ₃ ^b	CNDO	$P_{\nu}^{\mu(2)} = \begin{bmatrix} -0.09 & 0 & 0 \\ 0 & -0.09 & 0 \\ 0 & 0 & -0.15 \end{bmatrix}$	$\begin{bmatrix} -0.02 & 0 & 0 \\ 0 & -0.02 & 0 \\ 0 & 0 & -0.02 \end{bmatrix}$	$\begin{bmatrix} -0.09 & 0 & 0 \\ 0 & -0.09 & 0 \\ 0 & 0 & -0.06 \end{bmatrix}$	$\begin{bmatrix} 0.01 & 0 & 0 \\ 0 & 0.01 & 0 \\ 0 & 0 & -0.07 \end{bmatrix}$						
		$P_{\nu}^{\nu(2)} = \begin{bmatrix} -0.39 & 0 & -0.04 \\ 0 & -0.40 & 0 \\ 0.05 & 0 & -0.61 \end{bmatrix}$	$\begin{bmatrix} -0.20 & 0 & 0 \\ 0 & -0.20 & 0 \\ 0 & 0 & -0.20 \end{bmatrix}$	$\begin{bmatrix} -0.08 & 0 & -0.01 \\ 0 & -0.06 & 0 \\ 0.00 & 0 & -0.39 \end{bmatrix}$	$\begin{bmatrix} -0.11 & 0 & -0.03 \\ 0 & -0.14 & 0 \\ 0.05 & 0 & -0.03 \end{bmatrix}$						
	Expt'l	$P_{\nu}^{\mu(2)} = \begin{bmatrix} 0.03 & 0 & 0 \\ 0 & 0.03 & 0 \\ 0 & 0 & -0.07 \end{bmatrix}$									
		$P_{\nu}^{\nu(2)} = \begin{bmatrix} -0.29 & 0 & -0.05 \\ 0 & -0.29 & 0 \\ 0.12 & 0 & -0.95 \end{bmatrix}$									

^aThe $P_{\nu}^{\mu(2)}$ and $P_{\nu}^{\nu(2)}$ tensors are given in coordinate system with the z' axes along the C-H(2) and C-F(4) bonds as shown in Figure 1(c) and 1(d), respectively. ^bThe $P_{\nu}^{\mu(2)}$ and $P_{\nu}^{\nu(2)}$ tensors are given in coordinate system as shown in Figure 1(e) and 1(f), respectively. The APTs of CHF₃ are taken from reference (18).

to the molecular structure.

Acknowledgement. This work was supported in part by the

Korea Science and Engineering Foundation.

References

1. W.B. Person and J. Overend, *J. Chem. Phys.*, **66**, 1442 (1977).
2. W.B. Person and G. Zerbi, Eds., "*Vibrational Intensities in Infrared and Raman Spectroscopy*", Elsevier, Amsterdam (1982).
3. J.H. Newton, R.A. Levine, and W.B. Person, *J. Chem. Phys.* **67**, 3282 (1977).
4. J. Morcillo, L.J. Zamarano, and J.M.V. Heredia, *Spectrochim. Acta* **22**, 1969 (1966).
5. W.B. Person and J.H. Newton, *J. Chem. Phys.* **61**, 1040 (1974).
6. K. Kim, *J. Phys. Chem.* **88**, 2394 (1984).
7. K. Kim, R.S. McDowell, and W.T. King, *J. Chem. Phys.* **73**, 36 (1980).
8. J.A. Pople and D.L. Beveridge, "*Approximate Molecular Orbital Theory*", McGraw-Hill, New York (1970).
9. W.J. Hehre, W.A. Latham, R. Ditchfield, M.D. Newton, and J.A. Pople, "*Quantum Chemistry Program Exchange*", QCPE **10**, 236 (1974).
10. C.E. Blom and A. Müller, *J. Mol. Spectrosc.* **70**, 449 (1978).
11. A.H. Wapstra and N.B. Gove, *Nucl. Data Tables* **A9**, 265 (1971).
12. H. Hirota, T. Tanaka, K. Sakakibara, Y. Ohashi, and Y. Morino, *J. Mol. Spectrosc.* **34**, 222 (1970).
13. R.C. Weast, Ed., "*Handbook of Chemistry and Physics*", CRC Press, Cleveland (1975).
14. M. Mizuno and S. Saeki, *Spectrochim. Acta* **A32**, 1077 (1976).
15. W.T. King and G.B. Mast, *J. Phys. Chem.* **80**, 2521 (1976).
16. W.B. Person and J.H. Newton, *J. Chem. Phys.* **64**, 3036 (1976).
17. K. Kim and W.T. King, *J. Chem. Phys.* **80**, 983 (1984).
18. K. Kim, *Bull. Kor. Chem. Soc.* **7**, 488 (1986).

Synthetic Studies on Penems and Carbapenems(IV). Practical Preparation of (3R, 4R)-4-Acetoxy-3-[(1R)-1-hydroxyethyl]azetid-2-one Derivatives from 6-Aminopenicillanic Acid

Yang Mo Goo* and Young Bok Lee

Department of Pharmacy, Seoul National University, Seoul 151

Ho Hyun Kim, Youn Young Lee, and Woo Young Lee

Department of Chemistry, Seoul National University, Seoul 151. Received October 6, 1986

Preparation of optically pure (3R, 4R)-4-acetoxy-3-[(1R)-1-hydroxyethyl]azetid-2-one derivatives, which can be employed as starting materials for synthesis of carbapenem and penem antibiotics, was established in high efficiency from 6-aminopenicillanic acid (6-APA). 6-APA was diazotized and brominated to give 6,6-dibromopenicillanic acid and its methyl ester was metalated with methylmagnesium bromide and condensed with acetaldehyde. The product, methyl 6-bromo-6-(1-hydroxyethyl)penicillanate was reduced with Zn-NH₄Cl-NH₄OH-acetone efficiently to give methyl 6-(1-hydroxyethyl)penicillanate, which was protected either with β,β,β-trichloroethoxycarbonyl group or with *t*-butyldimethylsilyl group. The thiazolidine rings of these compounds were cleaved by treatment of mercury(II) acetate in acetic acid and permanganate in acetone in sequence to afford the desired optically pure final products.

Introduction

After discovery of a carbapenem antibiotic, thienamycin (1)¹ and Woodward's report² on penems (2), much efforts have been focused on the synthesis of new nonclassical β-lactam antibiotics and on the establishment of their structure-antimicrobial activity relationships³. Our current interest in synthesis of new penem and carbapenem antibiotics demands us to develop a practical method for preparation of the stereochemically pure (3R,4R)-4-acetoxy-3-[(1R)-1-hydroxyethyl]azetid-2-one derivatives (3a and 3b). For the construction of penem or carbapenem structures, these azetid-2-one derivatives are good starting materials on many respects, since many well established methods for the

functionalization⁴ at the C-4 position of the azetid-2-one ring have been developed and the formation⁵ of fused azetidione bicyclic systems from these azetid-2-ones can be easily achieved.

There have been several reports on the construction of derivatives of 3-(1-hydroxyethyl)azetid-2-one. McCombie reported on the preparation of 3-(1-hydroxyethyl)-4-ethylthioazetid-2-one⁶ from 4-acetoxyazetid-2-one and also from 6-APA(4). The azetid-2-one derivative was used for the construction of a penem antibiotic, Sch 29482. Chemists at Merck & Co. described the preparation of 4-acetoxy-3-(1-hydroxyethyl)azetid-2-one from aspartic acid⁷ and 4-acetoxy-3-[1-(*p*-nitrobenzyloxycarbonyloxy)ethyl]azetid-2-one from 6-APA in a patent⁸. However, it